Firefly

Contract No. N00014-12-M-0097

Quarterly Progress Report

CDRL 0002AA (submittal 1)

Period Ending: May 29, 2012

Submittal Date: May 29, 2012

Program Manager

Ashok Maliakal

15 Vreeland Ave

Room 2-034

Florham Park, NJ 07932

Phone: 973 437-9855

Email: maliakal@lgsinnovations.com

Contract Manager

Mark Miller

15 Vreeland Ave

Room 2-117

Florham Park, NJ 07932

Phone: 973 437-9763

Email: millerm@lgsinnovations.com

Report Documentation Page

Form Approved
OMB No. 0704-0188

1. REPORT DATE	2. REPORT TYPE	3. DATES COVERED
JUN 2012		**00-00-2012 to 00-00-2012**

4. TITLE AND SUBTITLE	5a. CONTRACT NUMBER
Firefly	5b. GRANT NUMBER
	5c. PROGRAM ELEMENT NUMBER
6. AUTHOR(S)	5d. PROJECT NUMBER
	5e. TASK NUMBER
	5f. WORK UNIT NUMBER
7. PERFORMING ORGANIZATION NAME(S) AND ADDRESS(ES) **LGS Innovations LLC,15 Vreeland Road,Florham Park,NJ,07932**	8. PERFORMING ORGANIZATION REPORT NUMBER
9. SPONSORING/MONITORING AGENCY NAME(S) AND ADDRESS(ES)	10. SPONSOR/MONITOR'S ACRONYM(S)
	11. SPONSOR/MONITOR'S REPORT NUMBER(S)

12. DISTRIBUTION/AVAILABILITY STATEMENT
Approved for public release; distribution unlimited

13. SUPPLEMENTARY NOTES

14. ABSTRACT

15. SUBJECT TERMS

16. SECURITY CLASSIFICATION OF:			17. LIMITATION OF ABSTRACT	18. NUMBER OF PAGES	19a. NAME OF RESPONSIBLE PERSON
a. REPORT	b. ABSTRACT	c. THIS PAGE			
unclassified	**unclassified**	**unclassified**	**Same as Report (SAR)**	**21**	

1 Overview.

LGS is continuing its investigation of new methods for measuring the mobility within organic photovoltaics using a combination of magnetic resonance methods. The primary goal of our work is to understand carrier transport better within the complex environment of the bulk heterojuntion (see Figure 1). In this second quarterly report, LGS in collaboration with Hunter College has completed work on baseline measurements of relaxation times for pentacene at various temperatures in order to determine optimal temperatures for measuring relaxation rate as a function of doping. We have also repeated these measurements on pentacene samples at 2 different doping levels, quantifying spin density using EPR spectroscopy and spin counting. As predicted by our model, relaxation enhancement at 300MHz is a somewhat weak effect, and we anticipate a stronger effect at lower field. As such we are working to optimize our T_1-p (rotating frame) relaxation experiment which will allow us to access these lower field strengths. We have also initiated our study of PCBM, by investigating

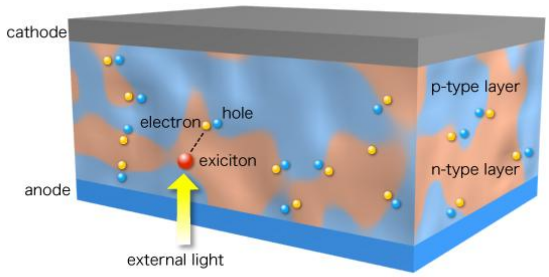

Figure 1: Schematic of Bulk Heterojunction (Adapted from Adachi Laboratory website, University of Kyushu). N and P type materials are co-deposited. Light absorption creates an exciton which migrates to the interface and dissociates into electron hole pairs. Electrons and holes must migrate to the electrodes quickly for efficient charge separation. The rate at which charge migration occurs is dictated by electron and hole mobilities.

the doping of this material with 4-(1,3-dimethyl-2,3-dihydro-1H-benzoimidazol-2-yl)phenyl)dimethyl amine (N-DMBI) using EPR spectroscopy. Preliminary NMR spectral data is promising for this system, since fast rotation of the fullerene in the solid state speeds up relaxation, which results in shorter T_1 relaxation times, which may allow for faster data collection. As a result C13 relaxation may be possible in this system at reasonable experiment times. In the case of P3HT, we have employed attenuated total reflectance ATR-IR spectroscopy to successfully calculate the diffusion constant for I_2 within P3HT using a time-lag method.

2 Technical Accomplishments This Period

Relaxation Measurements on Pentacene.

As described initially in the 1Q report, when magic angle spinning is employed, no paramagnetic relaxation enhancement is observed when comparing doped and undoped pentacene. This is demonstrated in Figure 2. The saturation recovery did not occur with mono-exponential kinetics; however an average relaxation time T_1 is estimated to be approximately 150-200s for both samples. The absence of a doping effect with MAS is consistent with the proposed mechanism for relaxation enhancement at high field, which is dipolar in nature and averaged out by the magic angle spinning. For this reason, for high field experiments, the saturation recovery experiment was performed without spinning.

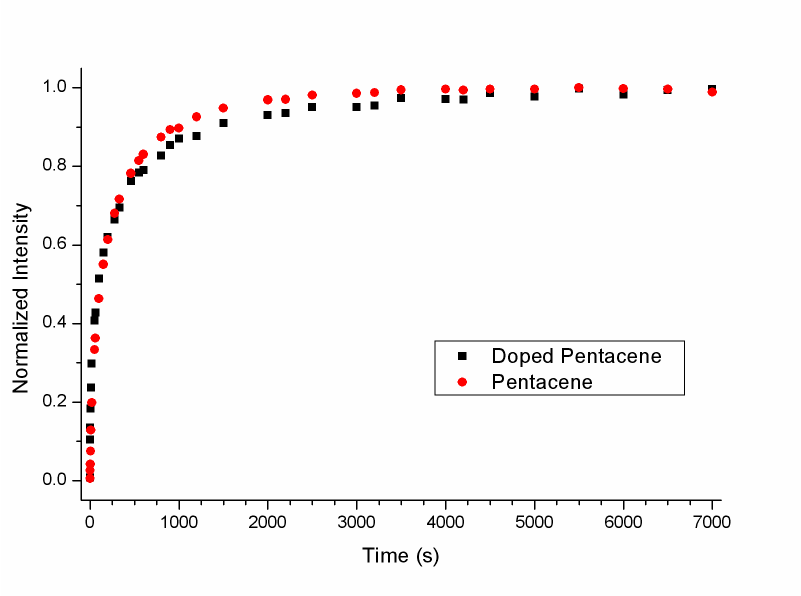

Figure 2. Comparison of Doped and Undoped Pentacene at 300MHz with Magic Angle Spinning.

Spin Counting for Pentacene. EPR spectroscopy was used to quantify spin densities within iodine doped pentacene. Copper sulfate was used as a standard, and a standard curve using known quantities of copper sulfate was generated comparing the amount of copper sulfate with the double integral of the copper sulfate EPR spectra. This standard curve was used to calculate spin density for doped pentacene EPR spectra. These data are tabulated in Figure 3.

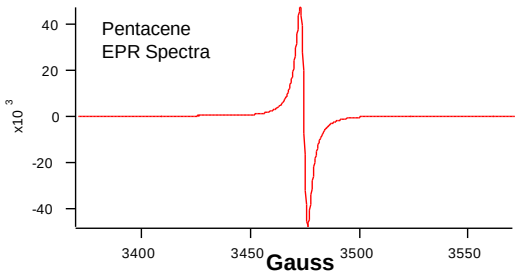

Sample	Spin Density (mol %)
Undoped Pentacene	0%
Lightly doped	0.17%
Highly doped	2.47%

Figure 3. Spin Counting Data for Pentacene.

Results for Undoped Pentacene. Initial data for undoped pentacene was presented in Q1 report, and since then, we have completed low temperature data for undoped pentacene (at -100 and -125 ˚C). The complete temperature vs. T_1 data set for undoped pentacene is presented in Figure 4. As can be seen from Figure 4, the fastest relaxation times are between 0-50 C, with correspondingly slower relaxation times at higher and lower temperatures.

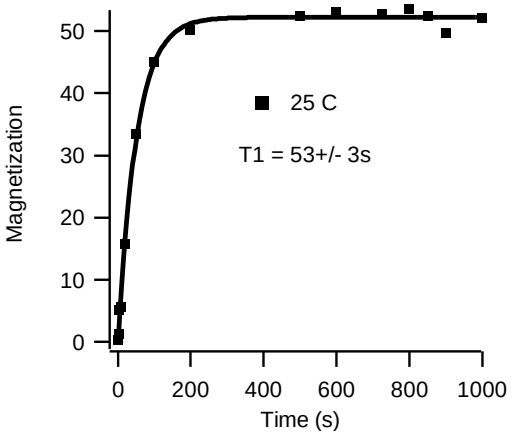

Temperature (°C)	T_1 (s)
150	96 ± 8
100	75 ± 10
50	54 ± 5
25	60 ± 10
0	56 ± 2
-25	72 ± 2
-100	107 ± 4
-125	123 ± 3

Figure 4. Undoped Pentacene. Example of typical saturation recovery data and table of baseline T_1 relaxation times vs. temperature.

When the sample is not spun, linewidths are quite broad, especially in the case of proton NMR. The linewidth for this sample vs. temperature is presented in Figure 5.

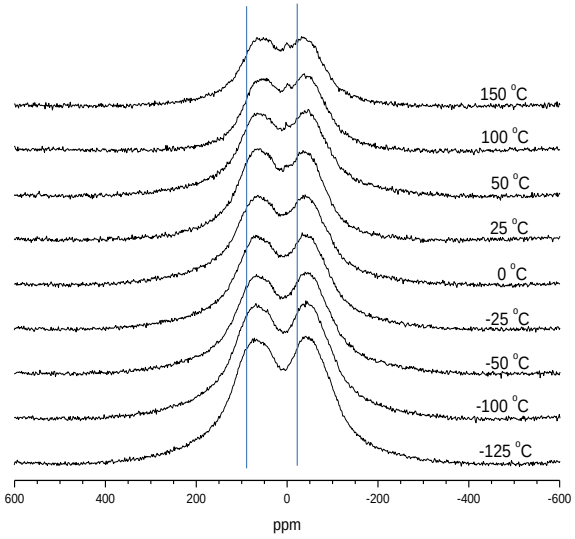

Temperature (°C)	FWHM (kHz)
150	57
100	59
50	60
25	60
0	60
-25	63
-50	67
-100	68
-125	72

Figure 5. Linewidth for Undoped Pentacene verses Temperature.

Results for Doped Pentacene.

NMR measurements of T_1 relaxation time for lightly doped pentacene (0.17% dopant) were taken for non-spinning samples from -100 to 150 C. These data are presented in Figure 6. In the case of the lightly doped sample, slightly shorter relaxation times are observed and the fastest relaxation times are observed at 25-50 C.

Linewidths are broad for the lightly doped pentacene, but narrower than that observed in undoped pentacene. The linewidth for lightly doped pentacene vs. temperature is presented in

Figure 7.

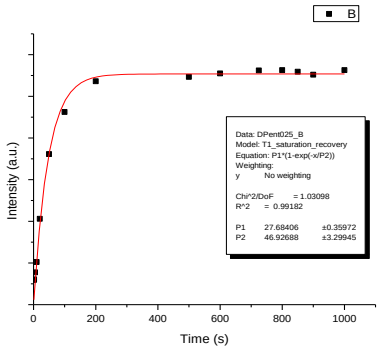

Temperature (°C)	T_1 (s)
-100	122 ± 4
-50	92 ± 3
-25	78 ± 3
0	66 ± 3
25	47 ± 3
50	47 ± 3
100	59 ± 4
150	103 ± 4

Figure 6. Relaxation Data for Lightly Doped Pentacene Sample (0.17mol% spins).

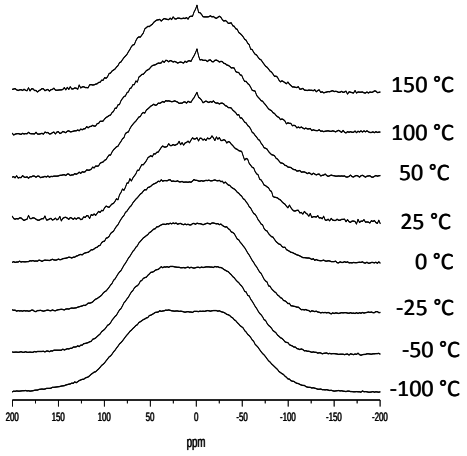

Temperature (°C)	FWHM (kHz)
150	46
100	47
50	48
25	47
0	48
-25	49
-50	48
-100	50

Figure 7. Linewidth vs. Temperature for lightly doped pentacene sample.

Similar NMR measurements of T_1 relaxation time were made for the highly doped pentacene sample. In the case of the highly doped sample, we see a more complex bi-exponential saturation recovery (see Figure 8).

A.

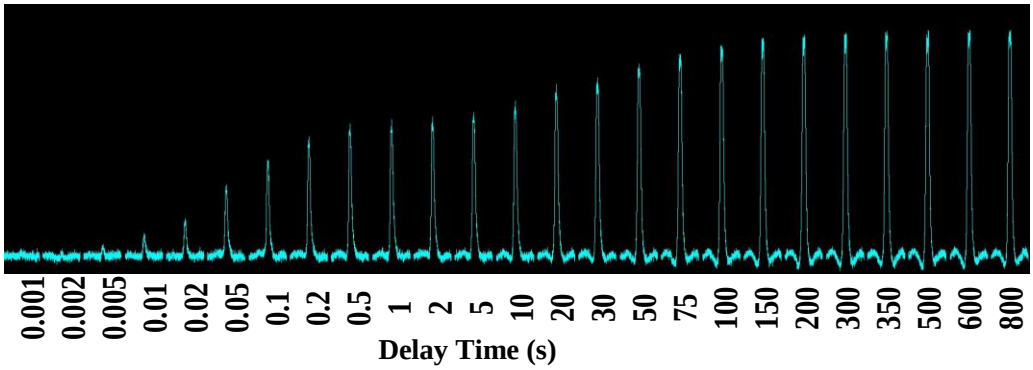

B.

Temperature (°C)	T_1 (s)	Fraction of Signal	T_1 (s)	Fraction of Signal
25	.085	0.46	47	0.54
50	.085	0.46	48	0.54
100	.060	0.45	43	0.55
150	.058	0.47	48	0.53

Figure 8. Relaxation Data for highly doped pentacene. A. Spectra taken from saturation recovery experiment with time delay listed. B. Summary of T_1 relaxation times and fraction of signal for temperatures ranging from 25-150C.

As can be seen from the Table in Figure 8, there is a very fast relaxation which ranges from 58-85 ms over the temperature range from 25-150C. There is also a slower relaxation which ranges from T_1 = 43-48s over the same temperature range. The fraction of each population appears relatively constant over the temperature range suggesting that the local environment for each species does not change over this temperature range. Based on data from the literature for iodine doped pentacene (see Brinkmann et. al. J. Phys. Chem. A., 2004), when pentacene is doped with iodine, at low doping levels no change in the crystal structure is observed. However at higher doping levels, a new crystalline phase is observed in which pentacene is intercalated by an iodine layer. The new phase has a crystalline layer spacing consistent with the iodine

intercalation. At very high iodine loading levels, the pentacene becomes amorphous. Our data suggests that we are beginning to see two different pentacene environments, and these could possibly conform with the environments observed by Brinkmann et. al. using x-ray diffraction as a probe. In the coming quarter we will attempt x-ray diffraction to probe the structure of pentacene.

Comparison of NMR Data from Pristine and Doped Pentacene.

Data collected for undoped pentacene and pentacene at both doping levels are presented together in Figure 9. The data is presented as relaxation rates ($1/T_1$) with units (s^{-1}). As can be seen from Figure 9, the relaxation rate maxima appear to shift to higher temperatures as a function of doping, although the data is still preliminary and low temperature measurements for the highly doped pentacene have not yet been performed. In the case of the highly doped sample, the data is presented for only the slow relaxing component, since the fast relaxing component has a relaxation rate ~10 s^{-1} which is roughly 2 orders of magnitude higher than the relaxation rate measured for the lightly doped and undoped samples. These experiments will be repeated in the next quarter to confirm that the results presented are reproducible. The data confirms that at 300 MHz, the paramagnetic relaxation enhancement due to mobile spins is primarily dipolar and weak (15-30%) in the case of the lightly doped sample, and 28-100% in the case of the highly doped sample (slow component), with more significant enhancement at higher fields. Note that at 100˚C, the doping appears to cause a monotonic increase in relaxation rate. More data points in this region may be useful for calculating relaxivity for the radical cation within doped pentacene.

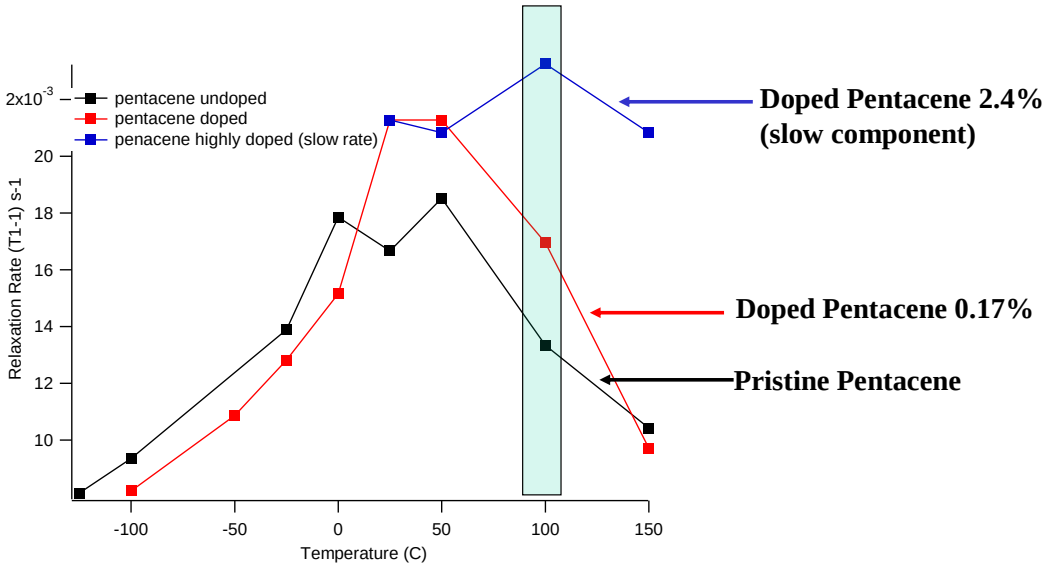

Figure 9. Relaxation Rate Data for pristine and doped pentacene.

Comparison of Linewidth Data:

Linewidth data for undoped and lightly doped pentacene are presented in Figure 10. As can be seen, the doped pentacene sample exhibits a narrower linewidth across the temperature range measured.

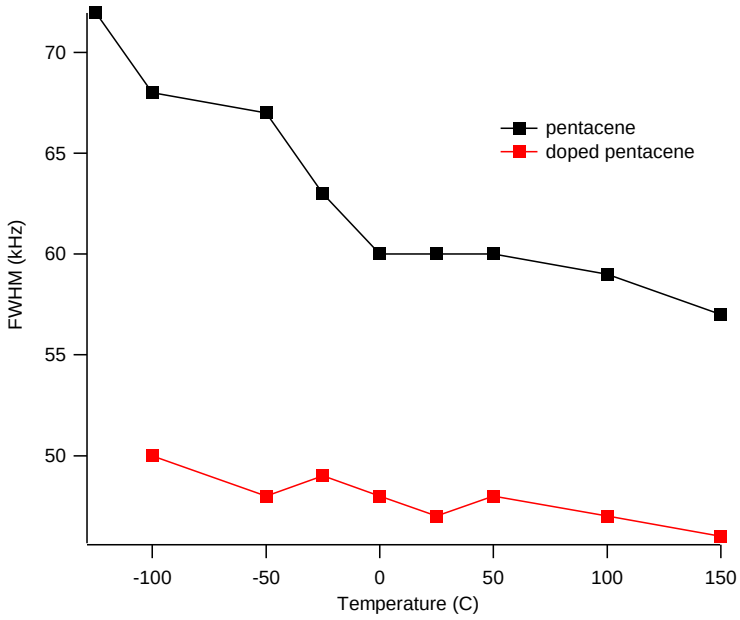

Figure 10. Linewidth data comparing pristine pentacene and lightly doped pentacene.

Initial Investigation of PCBM Doping.

In the past quarter we have begun our investigation of PCBM with initial NMR data collected and also evaluation of the effect of a new dopant 4-(1,3-dimethyl-2,3-dihydro-1H-benzoimidazol-2-yl)phenyl)dimethyl amine (N-DBMI). Initial EPR data has been taken on PCBM as received from Aldrich, and a PCBM/N-DMBI blend (2% N-DMBI) both as cast, and also after 1 and 2 hours of thermal treatment (100 ˚C). The dopant N-DMBI was introduced by Z. Bao's group (Wei, Bao, et. al., J. Am. Chem. Soc. 2010) as an electron dopant for PCBM. The N-DMBI is cast along with the PCBM from chlorobenzene, and as cast is not reported to have a doping effect. The doping is affected only as a result of thermal annealing (80˚C overnight in the Wei, Bao work); in our work, the samples were heated for 1-2 hrs at 100˚C.

The proposed mechanism for N-DMBI action is via homolytic cleavage of the benzylic hydrogen followed by electron transfer (Wei, Bao, J. Am. Chem. Soc. 2010) (see Figure 11). However there is ongoing debate and unpublished experimental data which contradicts this mechanism (personal communication with Seth Marder, Georgia Tech).

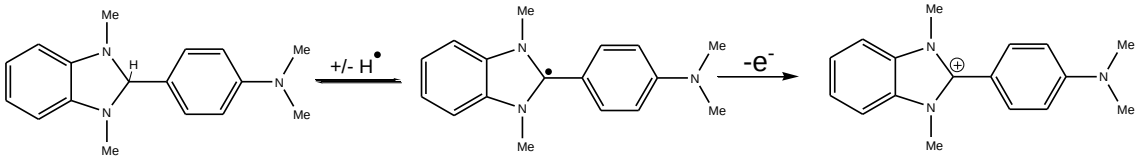

Proposed doping mxn. (P. Wei, Z. Bao, J. Am. Chem. Soc. 2010)

Figure 11. Mechanism for electron doping of PCBM by N-DMBI.

In initial EPR investigations of this system, N-DMBI (2 weight%) and PCBM were dissolved in chlorobenzene and after stirring, the solvent was permitted to evaporate, leaving behind a film of the PCBM with 2% N-DMBI. EPR of the N-DMBI, PCBM as received and PCBM mixed with 2%

DMBI are presented in Figure 12.

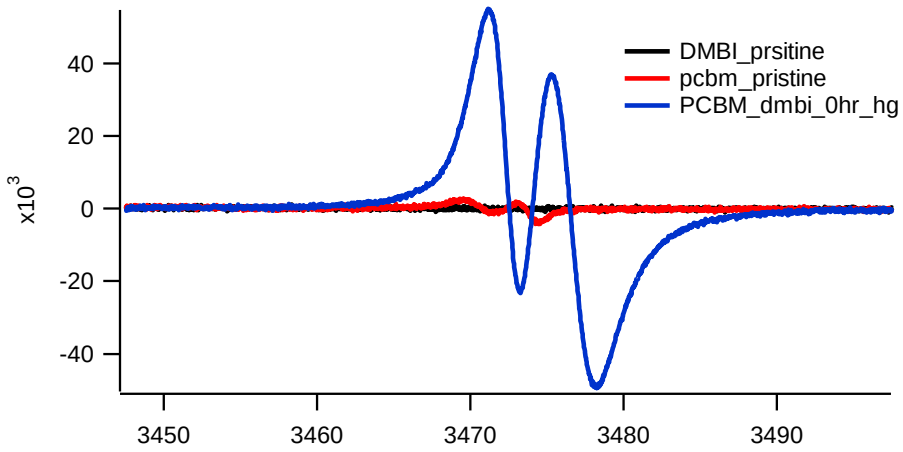

Figure 12. EPR Spectra for N-DMBI (black), PCBM as received (red), and PCBM/DMBI mixture after casting.

As can be seen, even without heating there is a significant increase in EPR signal for the mixture of PCBM and 2% DMBI. After heating for 1 hour, the EPR spectra for PCBM/DMBI increases further by roughly 1 order of magnitude(see Figure 13). However measurements made after 2 hrs of heating show a dramatic decrease in signal intensity (reducing by more than 1 order of magnitude), suggesting some degradation process for removing spin density from the sample. All heating steps were carried out in inert argon environment, samples were capped in inert environment before transferring to EPR spectrometer. The relative signal strengths for the different samples are presented in Figure 14. We are further investigating these interesting doping results.

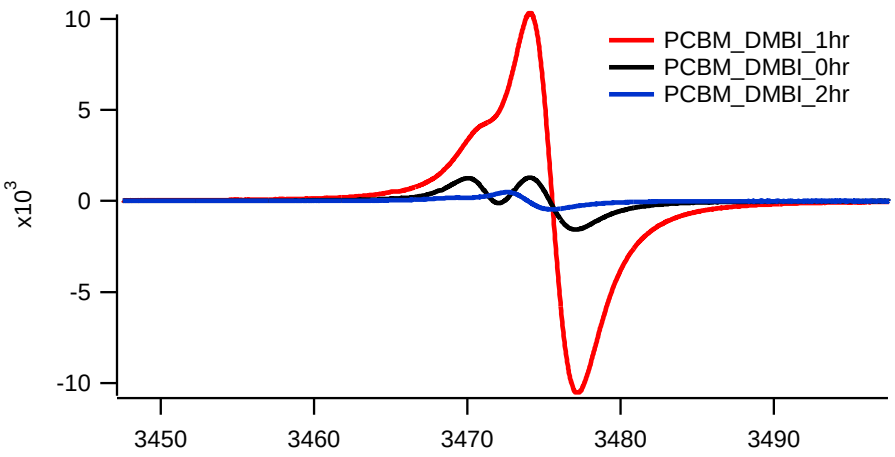

Figure 13. PCBM/ DMBI mixture after casting (black), after 1hr heating at 100 C (red), and after 2 hrs heating (blue).

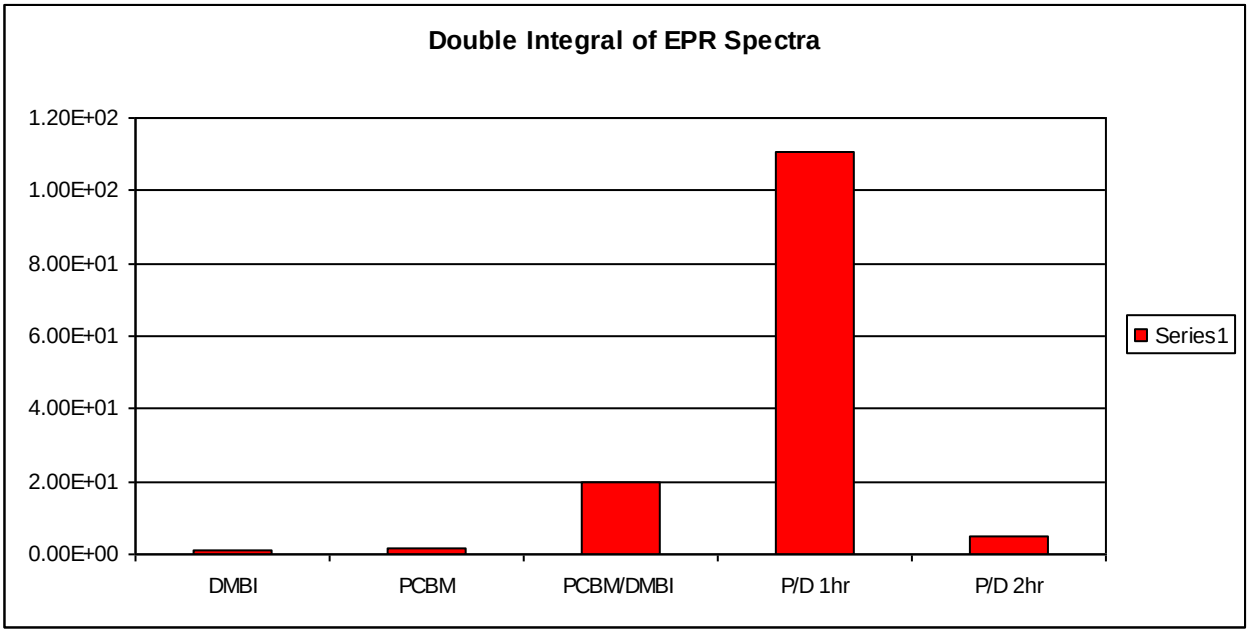

Figure 14. Summary of EPR data for PCBM/N-DMBI mixtures.

In anticipation of T_1 relaxation measurements for PCBM/N-DMBI mixtures to investigate the effect of doping on relaxation for PCBM, we have taken preliminary solid state MAS-NMR spectra for these compounds and mixtures presented in Figure 15. With spinning, significantly

narrower linewidths are achieved. In the case of PCBM, since relaxation times for this material are shorter due to rotational motion in the solid state, spectra can be taken in reasonable timeframes opening up the possibility of ^{13}C T_1 measurements in this system. In the next quarter we will pursue relaxation rate measurements on PCBM as received, and PCBM doped using DMBI.

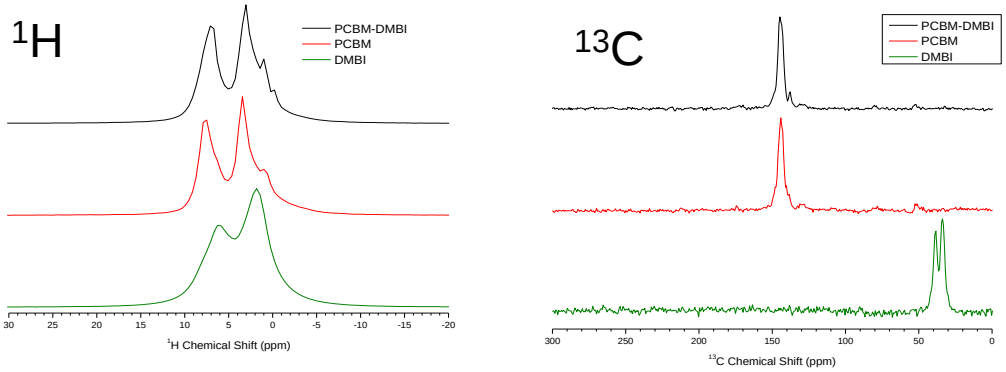

Figure 15. NMR Data for PCBM, DMBI and PCBM/DMBI mixture (2% DMBI).

Experimental Section

Proton nuclear magnetic resonance (^1H NMR) experiments were performed at Hunter College using a 7.1 T magnet and Varian Direct Drive S spectrometer. Static measurements were conducted on a single-channel home-built low proton-background 5 mm probe. Polycrystalline pentacene (Sigma Aldrich) was packed into a glass NMR tube and capped with Teflon tape. A radiofrequency field strength of approximately 20 kHz ($\pi/2$ = 13 μs) was used for excitation. A single transient using direct excitation was used to collect data at temperatures ranging from -25 °C to 150°C. Spin-lattice relaxation (T_1) measurements were conducted using a saturation recovery sequence in the above temperature range. A total of 25 $\pi/2$ pulses separated by 200

μs were used to saturate the signal. Four transients were collected for each arrayed time value in the saturation recovery sequence. Exponential broadening was applied to the signal prior to Fourier transformation and the subsequent spectra were base line corrected. The integrated intensities were then taken and fitted to a single exponential using OriginPro 7.0.

For magic angle spinning (MAS) NMR measurements, a Varian 1.6 mm HX probe was utilized. The sample was spun at a spinning rate ν_r = 36 kHz. Data were collected using a single pulse sequence and a single transient, employing a recycle delay between 100 – 800 s and a radiofrequency field strength of approximately 150 kHz ($\pi/2$ = 1.7 μs).

Dopant Diffusion within P3HT using ATR-IR.

In the previous quarter, initial investigation was made into the ability of attenuated total reflectance IR spectroscopy (ATR-IR) to probe the diffusion of iodine dopant within P3HT. The presence of iodine within P3HT results in the formation of polarons, and these polarons have intense absorption bands. (Heeger, A.; Kivelson, S.; Schrieffer, J.; Su, Rev. Mod Phys. 1988, 60, 781) A broad absorption band is observed at ~3500 cm^{-1} in addition to several more bands in the 1000-1500 cm^{-1} region.

Our experiment takes advantage of the ability of ATR to probe only a small depth within the sample film deposited on the IR transparent cell material as a result of the rapid decay of the evanescent wave. (see Figure 16). The critical equation defining penetration depth (DP) (Thermo Electron ATR-cell manual) is given below:

$$DP = \frac{\lambda}{2\pi n_1}\left[\sin^2\theta - \left(\frac{n_s}{n_1}\right)^2\right]^{-\frac{1}{2}}$$

In this case λ is the wavelength, n_1 is the refactive index of the IR medium, n_s is the refractive index of the sample, and θ is the angle of incidence which for our sample cell is 45˚. In the case of P3HT, the refractive index is approximately 1.6 – 1.7. A necessary condition for this experiment to work properly is described below (condition for total internal reflectance):

$$\sin^2\theta \succ \left(\frac{n_s}{n_1}\right)^2$$

In order to get narrow pentration depths that are not terribly sensitive to the value of n_s it is good to have n_s/n_1 as small as possible. This condition is achieved using germanium as the IR medium (germanium $n_1 = 4$). In this case, penetration depths range from 540 m for 1310 cm^{-1} to 180 nm for 3950 cm^{-1}. For a significantly thicker film, this limits the detection zone, so that diffusion measurements can be made using the time lag approach.

In our experiment a film of P3HT is deposited on the IR medium using drop casting (film thickness 5-10 um). The film is annealed for 30 mins at 100C. After cooling the film is transferred to the IR spectrometer. Baseline IR spectra prior to doping is taken. After this step, a small vial containing iodine crystals is introduced into the IR cell. (the cell is covered with a glass cap, to prevent iodine vapors from diffusing throughout the spectrometer). In order to facilitate rapid equilibration of iodine vapor, the iodine crystal is heated to 50˚ C prior to transfer to the IR cell. IR spectra are taken as a function of time for approximately 1 hour with samples taken approximately once per minute.

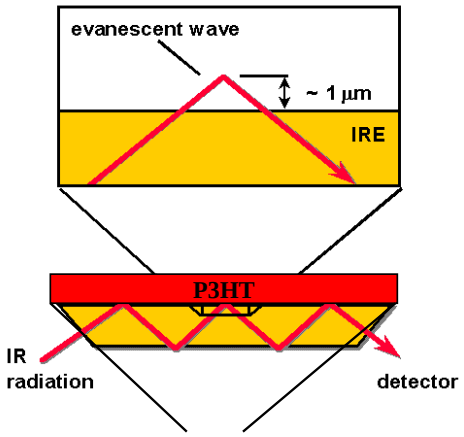

Figure 16. Scheme for P3HT deposited on IR mirror. Inset shows depth of pentration due to evanescent wave.

Typical data for P3HT films on germanium is presented in Figure 17. Since the absorption for the polaron resulting from iodine doping is broad, we can monitor at several different wavelengths simultaneously in order to calculate the diffusion coefficient. When the absorption is plotted versus time, the data is consistent with Fickian diffusion, and show a transient region followed by linear region where a constant flux of diffusive species accumulates within the detection region (see Figure 18). In this approach to measuring diffusion constants, the x intercept for the linear region can be used to calculate the diffusion coefficient using the equation from Figure 18. Representative data for diffusion of iodine through P3HT is presented in Figure 19. From this data, for this particular film, a diffusion coefficient of 4.7+/-0.35 x$10^{-11}$$cm^2$/s is calculated using the equation from Figure 18. Within a given film, data tends to be reasonably consistent. There is still some degree of variability for measured diffusion when different films are tested. Averaging measurements from 3 films ranging from 5-10 µm thickness, we get an average diffusion constant for I_2 D_{avg} = 9 +/- 5 x10^{-11} cm^2/s. We believe these variations may be due to difference in the film processing or environment (ex.

Humidity may play role, thicker films may be more likely to crack on annealing allowing faster diffusion). Further experimentation in the coming quarter should provide insights into these variations.

Finally in comparison with previous literature on oxygen diffusion within P3HT, Abdou et. al. have reported 1.2 $x10^{-8}$ cm^2/s as the diffusion coefficient for O_2 through P3HT (Abdou et. al. J. Am. Chem. Soc. 1997, 119, 4518-4524). This paper also used the time delay method to measure diffusion coefficient. However the detection was made by measuring partial pressure of oxygen across a P3HT membrane as a function of time.

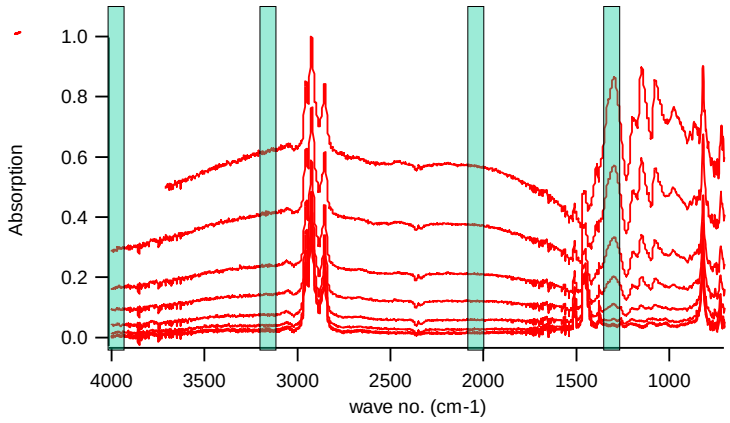

Figure 17. IR spectra for P3HT of Germanium medium. Data collected over ~ 1 hour. Each blue band represents a window which was used to measure signal strength versus time in order to calculate diffusion constant.

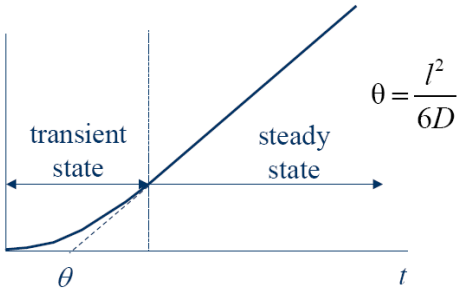

Figure 18. Time Lag method for measuring diffusion through a polymer film. (adapted from lecture notes of Dr. Jim Elliot, "Diffusion in Polymers", 2004)

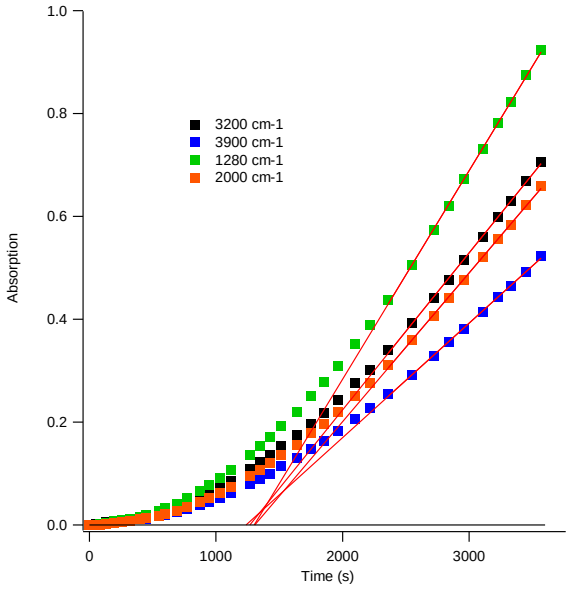

Figure 19. Absorption of P3HT vs. Time after iodine vapor exposure at different frequencies, showing increase due to polaron resulting from doping. Red lines are linear fits for linear portion of data. X-intercept is used to calculate diffusion coefficient for iodine in P3HT.

3 Anticipated Activities Next Period

In the next quarter, we will work to debug the T1-p experiment so that we can begin measuring

relaxation in the rotating frame, as we hope to observe a more dramatic enhancement effect under these conditions. We will make these measurements on the pentacene system, and expand our measurements to the PCBM system. We will further pursue optimal DMBI doping conditions for PCBM. We will work on getting more reproducible results for the measurement of I2 diffusion within P3HT, and expand these measurements to P3HT/PCBM system. We hope to publish these diffusion results soon, and will work to get these data to the level for peer review.

4 Contributors

Ashok Maliakal (LGS Innovations, LLC.), Paul Sideris and Steve Greenbaum (Hunter College).